ISSN 1063-7745, Crystallography Reports, 2019, Vol. 64, No. 3, pp. 515–523. © Pleiades Publishing, Inc., 2019.
Russian Text © The Author(s), 2019, published in Kristallografiya, 2019, Vol. 64, No. 3, pp. 484–493.

CRYSTALLOGRAPHIC METHODS IN HUMANITARIAN SCIENCES

X-Ray, Synchrotron and Mass-Spectrometric Methods for the Study of Ceramic Objects of Cultural Heritage

A. M. Antipin[a,*], V. B. Kvartalov[a], R. D. Svetogorov[b], A. Yu. Seregin[a,b], N. F. Fedoseev[c†], E. Yu. Tereschenko[a,b], O. A. Alekseeva[a], and E. B. Yatsishina[b]

[a] *Shubnikov Institute of Crystallography, Federal Scientific Research Centre "Crystallography and Photonics," Russian Academy of Sciences, Moscow, 119333 Russia*

[b] *National Research Centre "Kurchatov Institute," Moscow, 123182 Russia*

[c] *Institute of Archaeology of Crimea, Simferopol, 295007 Russia*

**e-mail: antipin@physics.msu.ru*

Received December 18, 2018; revised December 18, 2018; accepted December 25, 2018

Abstract—Fragments of stamped amphorae (south Pontic (Sinope, III–I BC) and Mediterranean (Thasos, IV–III BC, and, presumably, Chios, III–II BC)), found in excavations on the Crimean Peninsula, have been investigated using X-ray diffraction, generalized semiquantitative X-ray fluorescence analysis, and inductively coupled plasma mass spectrometry. The data obtained have been subjected to comparative analysis. A comparison of the mineralogical and elemental compositions of samples has revealed the characteristic distinctions between the products fabricated at different ancient pottery centers.

DOI: 10.1134/S1063774519030039

INTRODUCTION

Clay has been widely used in production of ceramic dishes and working tools, civil engineering, medicine, and other fields of human activity since the ancient times. Ceramic products, which have been generally preserved well up to present, serve a source of valuable historical information. A characteristic feature of ancient epoch was stamping pottery (especially standardized ceramic material) by manufacturers' stamps. Close trade, technological, and cultural relations between the ancient production centers led to active commodity exchange. For this reason, numerous ceramic products from the North Black and Mediterranean polises (Sinope, Trebizond, Thasos, Chios, Knidos, etc.) are found on the Crimean Peninsula, which became a territory of several Greek colonies as a result of Great Greek colonization in the period of VII–VI BC. Note that, along with stamped products, archaeologists often find fragments of ceramic artifacts without stamps, i.e., of unknown origin (production site and time), and there is a problem of their attribution. Traditionally archaeologists determine the site of mass pottery production by comparing the shape of vessels or their shaped parts, as well as the specific features of the ceramic mass they are made of (color, density, porosity, inclusions in clay, etc.). In particular, according to the data of [1], Sinope amphorae are characterized by a highly homogeneous composition of mineral additives in the molding mass (basically pyroxenes). However, the determination of the origin of ceramics and its dating on the basis of only macroscopic characteristics is hypothetical in many cases. Therefore, even in the end of the 1950s [2], researchers began to use the methods and approaches of physical materials science in order to obtain more exact quantitative data and reveal stable features of the clay molding mass composition.

Our purpose was to develop and approve a technique for parameterizing ceramic samples using the data on the phase and elemental compositions, up to trace impurities. In this paper, we report the results of a complex investigation of the fragments of ancient amphorae (IV–I BC), found on the Crimean Peninsula, by X-ray fluorescence (XRF) analysis, X-ray diffraction (XRD) analysis, and inductively coupled plasma mass spectroscopy (ICP-MS).

OBJECTS AND METHODS OF STUDY

To carry out a complex natural science study, we chose fragments of six ancient ceramic amphorae found on the Crimean Peninsula territory. The samples are dated to IV–I BC and have stamps of large clay production centers:

(S1) Sinope amphora (~250 BC);

(S2) Sinope amphora (~233 BC);

(S3) Pontic (late Sinope) amphora (II–I BC);

(Th1) Thasian amphora (~303–393 BC);

† Deceased.

(Th2) Thasian amphora (~350 BC);

(Ch1) presumably, Chiosian amphora (III–II BC).

In IV–III BC, the polises of South Pontus, including Sinope, played an important role in the trade between the North Black Sea polises. In the classical and Hellenistic times, workshops producing amphorae and tiles were located on the territory of modern district Zeitinlik of Turkish town Sinope. The dense clay paste of the Sinope amphorae is characterized by a lilacish hue, sometimes with yellowness; acute-angle lustrous dark inclusions of pyroxene can clearly be seen in it. Samples C1 with a stamp of magistrate Apollodorus, son of Dionysius, and a stamp of potter Thebeus on the second handle (~250 BC) and C2 with a stamp of magistrate Gill, son of Philisk, and potter Agatho (~233 BC) [3] originate from this region. Kilns of later period (II BC–VII AD) were discovered westward from Sinope, near Demerdzhi. Sample C3 with an unknown stamp on the neck belongs to this group [4].

The Greek island Thasos in the Aegean Sea was a famous wine-making center. Stamped amphorae with wine had been delivered to Bosporus beginning with the V BC. Thasian amphorae are characterized by a reddish clay paste, with many fine-grained lustrous inclusions of mica. Excavations were performed in only in 5 from 16 pottery workshops discovered on Thasos; each workshop used its own clay mine to fabricate amphorae. We investigated fragments of amphorae with stamps of magistrates Polynevk and Cleitus: samples Th1 (~303–393 BC) and Th2 (~350 BC), respectively. Sample Ch1 (III–II BC), with an englyphic stamp in the form of ring on the neck, was presumably made on the Greek island Chios, with which Bosporus had intense trade relations from the end of VI to IV BC. The clay of these amphorae is dense and bright-brown, with few inclusions of sand, small white opaque calcic particles, and mica [5, 6].

From the point of view of materials science, ceramics is a multicomponent multiphase system [7], containing a clay base and artificial additives: nonplastic materials of organic or inorganic nature. This circumstance determines a wide variety of methods used to study ceramic artifacts [8–10]. Modern analytical methods make it possible to find the mineral and chemical compositions of molding mass, reveal specific features of fabrication technology, and even identify raw material sources [11–14].

One of the most important characteristics of clay material is its elemental composition. The data on the main and admixture elements and their concentrations play a key role in determining the regional affiliation of products, in some cases, up to a specific pottery workshop or raw material deposit [15]. An analysis of the elemental composition by the nondestructive XRF method makes it possible to detect a majority of chemical elements (from Si to U). An inestimable advantage of this method is the possibility of studying objects of various sizes: from the entire object to its individual fragments or microprobes. For this reason XRF is often applied in modern archaeological studies. In particular, Mn, Cr, Ni, Ti, and Zr impurities in the ceramic objects studied in [16] were used as markers of geological situation in the vicinity of Aiani (Northern Greece) ceramic workshops. It was suggested in [16] that the vessels were fabricated in a local workshop, and the essential differences in the composition are due to the significant variation in the local clays used by ancient potters (this region has a complex geological structure). The elemental analysis data obtained in [17] when studying the fragments of ancient amphorae found in the Black Sea ancient town Tanais threw discredit on the conclusions about the Herakleian origin of amphorae and showed similarity of their composition to the Sinope clay.

Another main method of clay diagnostics is XRD. This technique makes it possible to classify data on ceramic products according to their mineralogical composition, determine the characteristic features of the clay base and admixtures, and attribute artifacts to a particular production center [18–20]. In addition, the presence or absence of certain crystalline phases (e.g., calcite, illite, gehlenite, wollastonite, etc.) in a sample allows one to draw conclusions about the firing temperature of the objects studied, which is one of the most important characteristics of fabrication technology [21–25]. Sometimes the large number of crystalline or partially crystallized phases in a sample does not make it possible to determine unambiguously a specific mineral and only indicates to a group of minerals characterized by close distances between atomic planes. To solve this problem, an additional analysis of individual crystalline inclusions, selected from samples, was performed. Since their small size excludes diagnostics on laboratory diffractometers, synchrotron radiation (SR) was used.

Mass-spectrometric methods of analysis of elemental composition, which are typical of metallurgical or geological applications, have become increasingly popular for solving historical and archaeological problems [26–29]. Mass spectrometry makes it possible to determine even concentrations of trace elements, as low as 10^{-10}–10^{-12} wt %. To classify ceramic samples, researchers select the elements (most often rare-earth) characterizing the origin region of starting materials (clay and nonplastic minerals). For example, when studying the ceramic products from ancient Karelian settlements, the differences in the contents of Ti, V, Y, La, and Th [25, 28] or Nb, Zr, Ti, Li, and U [30] were taken into account. The researchers studying the ancient ceramics from the Koss island [31, 32] analyzed the differences in the Co, Sc, Cs, K, and Rb concentrations for one group of samples and the Co, Sc, U, Th, Sb, and La concentrations for the other group. Obviously, there is no universal list of admixures that could be used to localize unambiguously the

production region of ceramic artifacts. This is related to the difference in the formation conditions for layers of argillaceous minerals and the wide variety of admixtures (from wool and food waste to chamotte) added to the ceramic paste to modify its properties. Note that it is very difficult to classify ceramic products with respect to petrogenic compounds, such as SiO_2, Al_2O_3, TiO_2, etc., because their concentrations in argillaceous minerals from different deposits are very close [30].

Previously, samples S1–S3, Th1, Th2, and Ch1 were investigated (among other samples) in [33] using a complex of modern electron microscopy methods, including scanning and transmission/scanning electron microscopy in combination with energy-dispersive X-ray microanalysis. The data of [33] and results of this study made it possible to develop and optimize an approach to the study of ceramic objects of cultural heritage.

EXPERIMENTAL

The elemental composition of ceramic samples was first determined by the XRF method. The analysis was performed using SR on the station "X-Ray Crystallography and Physical Materials Science" of the unique facility "Kurchatov Synchrotron Radiation Source" (KSRS) at the National Research Centre "Kurchatov Institute" [34]. A monochromatic 18-keV X-ray beam excited fluorescence from the elements entering the sample composition. Fluorescent spectra were recorded using an energy-dispersive SDD detector Amptek X123. Each spectrum was collected for 1200 s. The composition of samples of arbitrary size was analyzed; the exposed area was 0.5×0.5 mm^2. Samples, mounted on a special holder, were oriented at an angle of 45° with respect to the incident beam. To exclude the influence of sample inhomogeneity, we averaged spectra recorded from three different regions for each sample. The fluorescent spectra and elemental composition of samples were analyzed applying the PyMCA program [35]. Since experiments were performed in air, light elements (up to Al) could not be detected. In the absence of standards, the XRF data can be considered as only qualitative. Semiquantitative values were obtained using normalization to the absolute values of iron concentration from the ICP-MS data for each sample.

X-ray diffraction analysis of ceramic fragments was performed on a laboratory powder diffractometer Rigaku Miniflex 600 (CuK_α, 8 keV) at the Federal Scientific Research Centre "Crystallography and Photonics," Russian Academy of Sciences. Diffraction patterns were recorded in the Bragg–Brentano geometry using a linear detector in the 2θ scan range from 2° to 75° with a step of 0.02°. Samples for studies were ground in an agate mortar and loaded in a quartz glass cell. The experiments and qualitative analysis of the phase composition were performed using the licensed package of MiniflexGuidance [36] and PDXL-2 [37] programs and the urgent powder database ICDD PDF-2. Quantitative analysis was carried out by the Rietveld method applying the Jana2006 software [38] and ICSD database.

An additional analysis of individual (the largest) inclusions of black, white, and beige colors, selected from samples S1, S2, and S3, was performed on the Belok station at the KSRS [39] using a monochromatic 12.78-keV beam. Samples were mounted on a cryoloop and rotated during measurements around the horizontal axis in order to average diffraction patterns over orientations. Diffraction patterns were collected in the transmission geometry using an area detector Rayonix SX165, located at a distance of 80 mm and oriented perpendicular to the SR beam. The sample–detector distance was calibrated applying a polycrystalline standard $Na_2Ca_3Al_2F_{14}$ (NAC NIST SRM) with known positions of diffraction peaks. Diffraction patterns were integrated according to the Fit2D program [40]. The phase composition was determined qualitatively and quantitatively using the Match! [41] and Jana2006 programs and urgent powder database PDF-4+, based on the method of corundum numbers [42].

The microelemental composition of ceramic samples was investigated using an iCapQ-c ThermoScientific mass spectrometer with ionization in inductively coupled plasma. Probes were prepared using deionized water (18 MΩ, Micropure); nitrogen (HNO_3 65%, EMSUREISO, Merck); hydrofluoric (HF 48%, EMSUREISO, Merck) and perchloric ($HClO_4$ 70%, ACROS) acids, certified for ICP-MS analysis; and a microwave autoclaving system CEM Mars 6. The samples were dissolved to the base concentration (0.1 g/L). The intensity was measured using the most widespread isotopes of analytes determined, free of isobaric overlaps. Polyatomic overlaps were corrected using a reaction collisional cell. Note that halogens, gas-forming elements, and some easily ionized elements (Na, K, Ca) cannot be characterized quantitatively by this technique. An internal standard, Bi and In solution (2 ppb), was used to monitor the influence of the matrix effect. Calibration, elemental analysis, and correction of spectral overlaps were performed according to the QTegra ThermoFisher program [43].

RESULTS AND DISCUSSION

A comparison of the fluorescent spectra (Fig. 1) revealed that all samples have a similar elemental composition. A qualitative analysis of the elemental concentrations showed that, along with the aluminosilicate matrix, the samples contain large amounts of Fe and Ca; the highest and lowest Ca concentrations are observed in samples S1 and S3, respectively. Admixtures of S, Cl, K, Ti, and Sr (more than

Table 1. Elemental composition of samples according to the XRF data (rel. wt %)

	S1	S2	S3	Th1	Th2	Ch1
S	0.571300	0.005545	0.006887	0.031660	0.002398	0.006868
Cl	0.151600	0.052830	0.002581	0.089200	0.026900	0.075260
Ar	0.088120	0.081250	0.050780	0.075210	0.033040	0.096150
K	0.183200	0.288700	0.270600	0.439700	0.516300	0.426100
Ca	2.560000	1.146000	0.718700	0.995200	1.566000	1.644000
Ti	0.070180	0.103100	0.105000	0.123600	0.130600	0.116000
V	0.005361	0.007226	0.007895	0.007007	0.008739	0.007507
Cr	0.004431	0.005341	0.011950	0.005599	0.006127	0.007690
Mn	0.083290	0.031470	0.024170	0.036320	0.032350	0.037870
Fe	2.302000	2.601000	2.601000	2.668000	2.979000	2.670000
Ni	0.011750	0.012520	0.012390	0.011450	0.010500	0.017100
Cu	0.002627	0.002640	0.002221	0.002567	0.002724	0.002999
Zn	0.014570	0.010100	0.007215	0.016630	0.011420	0.009817
Ga	0.001709	0.002169	0.001688	0.001967	0.002065	0.002424
As	0.000643	0.002430	0.000657	0.002071	0.003804	0.002300
Se	0.000040	0.000130	0.000022	0.000003	0.000011	0.000047
Br	0.003874	0.003433	0.000470	0.002765	0.001515	0.002206
Rb	0.017040	0.029810	0.024490	0.035420	0.026180	0.028260
Sr	0.081300	0.104000	0.077700	0.048900	0.034700	0.138000
Y	0.006662	0.007792	0.006032	0.009949	0.004764	0.007374
Yb	0.001425	0.001201	0.001016	0.001042	0.001525	0.001192
Lu	0.000654	0.000818	0.000499	0.000927	0.001044	0.000709
Re	0.000221	0.000118	0.000093	0.000444	0.000187	0.000566
Os	0.000161	0.000065	0.000085	0.000156	0.000294	0.000322
Au	0.000108	0.000133	0.000040	0.000016	0.000086	0.000028
Pb	0.000445	0.003230	0.012500	0.010950	0.005321	0.002645
∑	6.160000	4.500000	3.950000	4.620000	5.410000	5.300000

0.05 rel. wt %) were also found in the samples. Note that the maximum S and Cl concentrations (among all samples) were found in S1. The Sr content in the group of Sinope samples (S1–S3) is 2.5–3 times higher than in samples Th1 and Th2; sample Ch1 is characterized by the highest Sr content. Trace impurities (less than 0.05 rel. wt %) in the sample composition were as follows: V, Cr, Mn, Ni, Cu, Zn, Ga, As, Se, Br, Rb, Y, Yb, Lu, Re, Os, Au, and Pb.

The conditions of XRF experiments did not make it possible to detect Na, Mg, and O, the elements entering the clay base composition (according to the electron microscopy data on these samples [33]). The conditions for detecting a fluorescent signal from the aluminosilicate matrix of the sample clay base were not optimal: the incident X-ray energy was much above the absorption edge of these elements, and their fluorescence was intensively absorbed by air.

The XRD study on the samples made it possible to determine the main crystalline phases from the positions of the strongest diffraction maxima (Fig. 2). An analysis with application of the ICDD PDF-2 database showed that the strongest reflections in the diffraction patterns of all six samples correspond to quartz. In addition, the diffraction patterns of all samples contain peaks corresponding to feldspars (albite) and micaceous minerals (muscovite). Calcite peaks of different intensities were revealed in the diffraction patterns of five samples. Peaks due to gypsum were identified for samples S1 and Th2. The key distinction between the mineral compositions of the ceramic fragments under study is the presence of pronounced peaks corresponding to pyroxene group minerals

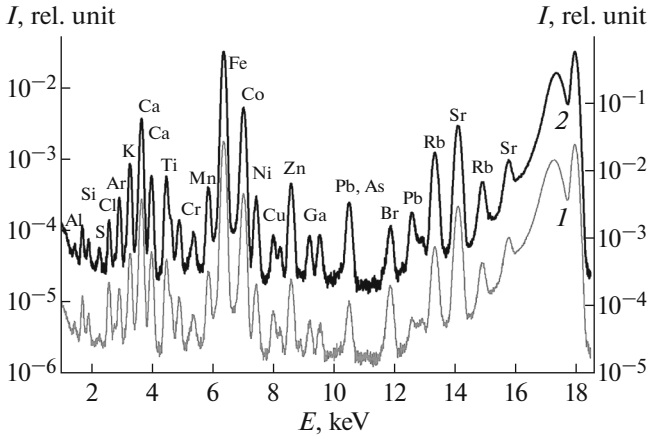

Fig. 1. Characteristic fluorescence spectra of (*1*) Thasos and (*2*) Sinope samples, averaged over groups.

(diopside) in the diffraction patterns of the three samples from the Sinope pottery center (S1–S3) and their absence in the samples of the Mediterranean group (Th1, Th2, and Ch1).

The initial data for quantitative (full-profile) analysis were the models of crystal structures from the ICSD database, corresponding to the previously found phases in the PDF-2 database. Refinement was performed via step-by-step addition of parameters (from the most stable to correlating) under constant graphical simulation of the background in order to stabilize *R* factors. The final values of the refinement parameters are listed in Table 2, and the data on the quantitative phase composition are given in Table 3. Some peaks were not correctly taken into account because of the mutual overlap and high background level. The spread of the percentage of XRD-identified phases in the samples from the same pottery center may be related both to small variations in the raw material composition or technological process in a wide time interval and to local changes in the concentrations of particular phases in different parts of vessel.

According to quantitative XRD data, the main mineral phases in both groups of samples are quartz (28–33%) and albite (26–44%). All six samples contain also muscovite in large amounts (up to 29%); its content in the Sinope samples is somewhat higher (Table 3). A full-profile analysis confirmed the high

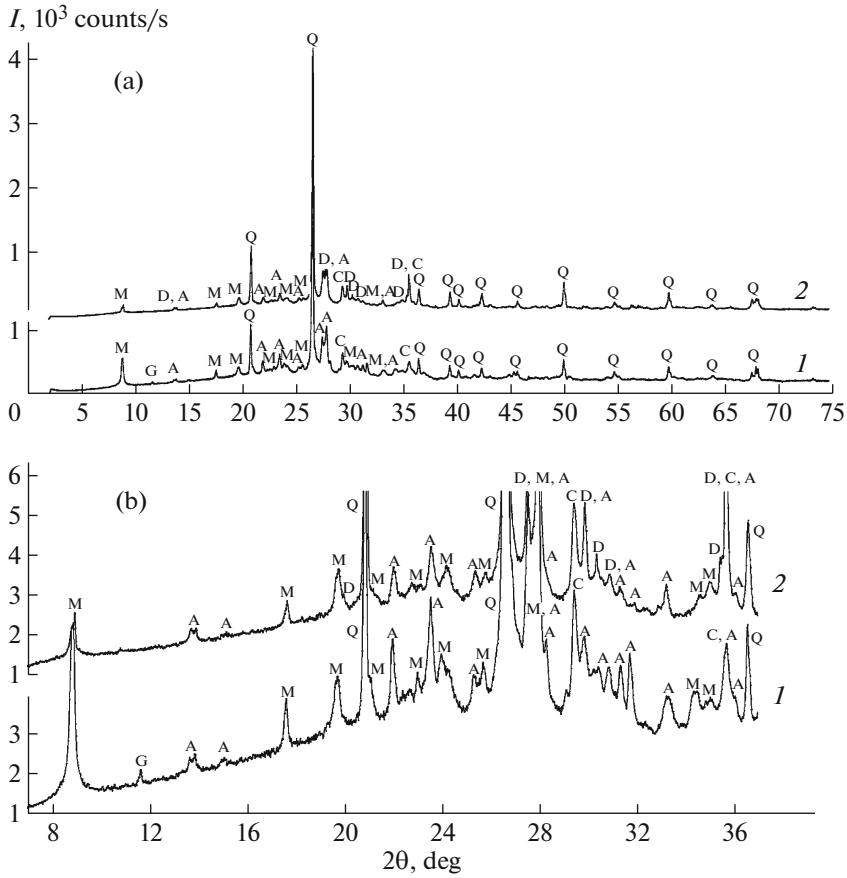

Fig. 2. X-ray powder diffraction patterns of samples Th1 and S1 in 2θ ranges of (a) 2°–75° and (b) 7°–37°. The designations as follows: (Q) quartz, (D) diopside, (A) albite, (M) muscovite, (C) calcite, and (G) gypsum.

Table 2. Final values of refinement factors according to the diffraction profiles

Refinement factors	S1	S2	S3	Th1	Th2	Ch1
S	5.26	5.11	5.31	5.50	6.02	4.48
R_p	7.06	6.81	7.04	7.07	7.29	6.27
wR_p	10.10	9.69	10.04	10.24	10.44	8.61

content (13–30%) of diopside in these samples, which is in complete agreement with the conclusions of [1]. The gypsum concentration in samples S1 and Th2 was 2%; however, among the identified phases, only gypsum contains sulfur in its elemental composition. According to the XRF data, the sulfur concentration is maximum in sample S1 and is much higher in Th2 than in other samples (Table 1). Note that gypsum, which is widespread in nature, can form layers or fine-grained aggregates in argillaceous sedimentary rocks [44]. Therefore, its presence (or absence) in ceramic products calls for a more careful consideration when

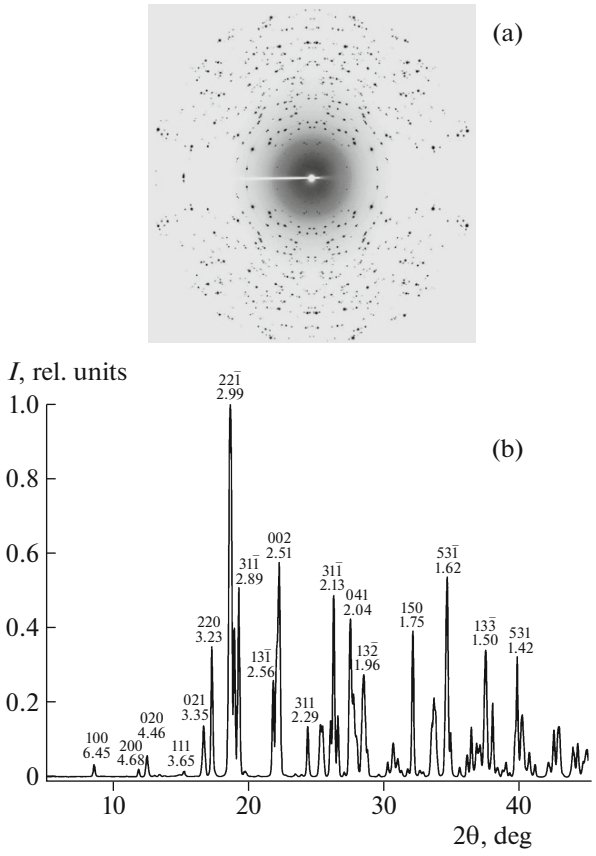

Fig. 3. (a) X-ray diffraction pattern and (b) results of phase analysis of a black inclusion from sample S2.

Table 3. Percentage of mineral phases in samples according to the quantitative XRD data

Sample	S1	S2	S3	Th1	Th2	Ch1
Mineral	Phase composition, wt %					
Quartz	28(3)	33(1)	29(3)	33(1)	37(1)	32(1)
Diopside	30(1)	23(1)	19(1)			
Albite	34(1)	31(1)	36(1)	28(1)	44(1)	26(1)
Muscovite	6(2)	9 (1)	18(3)	22(1)	14(1)	29(1)
Calcite		3(1)	2(1)	17 (1)	3(1)	13(1)
Gypsum	2(1)				2(1)	
Σ	100	100	100	100	100	100

determining the possibility of assigning this mineral to characteristic signs of a specific production center.

Another interesting feature is the presence of calcite in all samples, except for S1. According to the results of quantitative phase analysis, its content in samples Th1 and Ch1 is much higher (up to 17%), although the XRF data showed the Ca content to be sufficiently high in all samples and maximum in S1. According to the scanning electron microscopy data [43], the concentration of carbon entering the composition of $CaCO_3$ is higher by a factor of 3–5 in the Mediterranean samples than in the Sinope ones, which confirms indirectly the larger amount of calcite in them. This mineral in the form of sea shell fragments could be used by ancient potters as a nonplastic material; it could also be present in clay layers as a natural impurity. Calcite is known to thermally decompose into calcium oxide with release of carbon dioxide upon heating above 600–850°C [45]. The preservation of the crystalline calcite phase shows that amphorae Th1 and Ch1 were fired at temperatures below 600°C.

Since all samples studied were mixtures of many different minerals, we tried to select individual inclusions from samples and study them using SR. In particular, we investigated black, visually homogeneous inclusions in Sinope samples (S1–S3). Integration of diffraction patterns and subsequent structure interpretation showed unambiguously that these inclusions are diopside single crystals (Fig. 3). We also selected and investigated white inclusions, which turned out to be crystalline quartz, and beige strata on the surface, which were identified as fine-grained anatase. This mineral may also be present in small amounts in other samples; however, in view of the complexity and composite nature of experimental diffraction patterns, it was not revealed when processing and refining phases.

Absolute concentrations of 42 chemical elements were found by the ICP-MS method (Table 4). A statistical analysis of the entire dataset (Fig. 4) showed

Table 4. Impurity chemical composition of samples according to the ICP-MS data

Sample	S1	S2	S3	Th1	Th2	Ch1
Analyte	Concentration, μg/g					
^{7}Li	21.19959	28.30898	24.355145	31.15777	32.65983	31.47955
^{9}Be	1.170984	1.5225245	1.4758415	2.294479	2.067292	2.714435
^{11}B	150.5692	58.058825	141.67085	64.22465	54.69989	70.9878
^{24}Mg	3045.804	3938.8965	3313.795	2385.563	3477.005	2501.39
^{45}Sc	50.68485	65.2583	62.27468	41.15967	32.72641	35.17162
^{47}Ti	3235.075	3716.019	3650.5725	3877.588	3525.526	3576.265
^{51}V	124.6956	164.06525	176.12315	119.8047	114.4029	126.3659
^{55}Mn	501.458	577.67165	712.17575	763.6175	704.4897	733.4334
^{56}Fe	22798.01	26163.43	26290.845	29833.85	26666.17	26703.76
^{59}Co	14.81388	17.80768	18.214315	18.42016	19.10723	22.48039
^{60}Ni	71.38827	62.774345	80.82264	90.73047	67.30193	131.4487
^{63}Cu	25.04834	25.62603	30.456495	32.23652	33.01901	34.48581
^{66}Zn	63.34242	56.40586	61.97457	152.7993	97.71488	82.49805
^{71}Ga	10.62802	13.612895	13.88686	22.61103	19.61036	22.79452
^{72}Ge	7.958077	9.816469	10.195391	14.59978	13.03898	12.92333
^{75}As	4.196707	5.2754815	6.4986705	16.94921	21.2276	12.67616
^{78}Se	<DL	<DL	<DL	<DL	<DL	<DL
^{85}Rb	12.8608	15.55952	15.537345	36.38099	36.19358	25.48036
^{88}Sr	194.0645	184.54485	205.43405	117.4574	118.9963	397.4884
^{89}Y	1.257839	3.248056	1.3622555	1.133417	1.434978	1.080354
^{90}Zr	34.66497	44.00052	47.664995	23.89217	20.32925	47.85214
^{93}Nb	7.135233	8.343445	8.0307505	13.95099	12.44964	15.63554
^{97}Mo	<DL	<DL	28.40115	<DL	<DL	<DL
^{107}Ag	0.399934	<DL	<DL	0.246679	0.489774	0.299747
^{111}Cd	1.764132	<DL	0.379548	22.15954	26.37214	15.71013
^{118}Sn	1.67679	1.40484	1.3530735	2.954629	2.253503	3.889609
^{121}Sb	0.794232	0.541863	0.60217	2.087887	2.468487	1.55924
^{126}Te	<DL	<DL	<DL	11.55413	11.81698	<DL
^{133}Cs	0.405225	0.720521	0.454716	2.499245	2.777052	1.377168
^{137}Ba	158.805	229.2816	131.7015	347.6984	341.7464	262.8553
^{139}La	4.157391	6.255283	5.935671	6.029377	4.991748	6.176967
^{140}Ce	15.07202	26.374975	24.331285	40.3559	30.41213	43.15474
^{145}Nd	3.740725	6.0954525	5.3409565	5.599232	3.559074	4.439393
∑REE	26.32473	44.67984	40.25516	56.74365	42.26911	57.30188
^{178}Hf	1.145102	1.512641	1.6033955	0.887137	0.757997	1.7874
^{181}Ta	0.49751	0.561252	0.5409155	1.145867	0.977111	1.391173
^{182}W	2.770716	1.2815495	1.377661	2.952304	2.644754	3.476296
^{185}Re	<DL	<DL	<DL	<DL	<DL	<DL
^{205}Tl	0.02259	0.389726	0.351895	1.160522	1.123231	0.608911
^{206}Pb	10.90879	34.066265	19.73798	52.57289	56.06119	24.38644
^{232}Th	0.715668	1.5445275	1.0084205	3.176272	1.400551	1.359754
^{238}U	1.325886	1.7696745	1.8654135	2.746128	3.120218	4.178072

DL is detection limit.

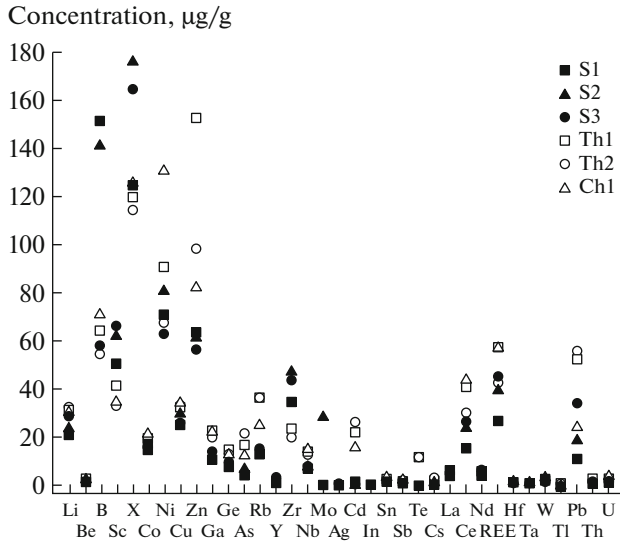

Fig. 4. Distribution diagram of chemical elements in samples according to the ICP-MS data (REE are rare-earth elements).

that the samples can be separated into two groups with respect to the content of different elements: S1–S3 and Th1, Th2, Ch1. Sample Ch1 differs from the Thasian samples mainly by the concentrations of Ni, Sr, and Ba. A comparative analysis showed that all clay samples have close contents of Ti, Fe, Mn, and Mg. However, the contents of some trace elements may significantly differ. In particular, the Mediterranean samples exhibited a twofold increase in the Ba concentration and a larger Zn content. Trace impurities of Li, Ga, Nb, Sn, Cs, Ce, Tl, Pb, and U were found in them, as well as Cd, which is practically absent in Sinope samples. The presence of Cd may be due to the existence of zinc or lead sulfides (Cd is often present in their minerals [46]) in the initial clay paste. The B, V, Zr, Hf, and Sr concentrations in Sinope ceramic samples differ significantly from the corresponding values for the Mediterranean group samples (Table 4). An exception is Ch1, where the Sr content greatly exceeds its concentration in other samples; this is in agreement with the XRF data. Despite the fact that XRD revealed the presence of mineral anatase (TiO_2) in sample S1, the titanium content in this sample remained the same, apparently, because of the presence of Ti in the clay base in the form of nanoparticles, detected by electron microscopy [43]. It was also found that the concentration of rare-earth elements in the Mediterranean samples exceeds that in Sinope samples (Table 4). The content of these elements is a parameter that is most often used for labeling ceramics in many studies [26–28, 30, 44]; the most descriptive markers are the Ce, Nd, and La concentrations [44]. Thus, despite the proximity of concentrations of widespread mineralogical impurities (Ti, Fe, Mn, Mg), the two groups of ancient ceramic products differ significantly in the contents of marker trace elements: Ga, Nb, Sn, Cs, Tl, Cd, B, V, Zr, Hf, Sr, and Ln.

CONCLUSIONS

Fragments of ancient amphorae (IV–I BC) found on the Crimean Peninsula were investigated using a complex of physicochemical methods: XRF, XRD, and ICP-MS. These methods, being reasonably supplementary, made it possible to investigate efficiently ceramic objects of cultural heritage having different origins.

Based on the studies of the fragments of ceramic amphorae having stamps of Sinope, Thasos, and Chios pottery centers, the elemental and mineralogical compositions and characteristic features of groups of samples were determined. The mineral composition of the Sinope group samples differs by a high content of diopside, small amount of muscovite, and almost complete absence of calcite (at a high total calcium percentage in the composition). The analysis of the mineral composition of Mediterranean samples, in contrast, did not reveal the diopside phase, and the muscovite concentration in them was much higher than in Sinope ceramics. The high calcite concentration in Mediterranean samples may indicate that these products were fired at low temperatures. Based on the data on the chemical composition of samples, one can say with confidence that the groups under study have different geochemical characteristics, which indicates that the raw materials from different deposits, differing in composition and genetic type, were used in ancient pottery.

It is proposed to use the above-described approach and set of determined physicochemical characteristics of ceramics from different pottery centers to localize the production sites for ceramic materials of unestablished origin.

ACKNOWLEDGMENTS

This study was performed using equipment of the Collective-Use Center "Structural Diagnostics of Materials" of the Shubnikov Institute of Crystallography, Federal Scientific Research Centre "Crystallography and Photonics" of the Russian Academy of Sciences, and the KSRS of the National Research Centre "Kurchatov Institute."

The study was supported in part by the Russian Foundation for Basic Research, project no. 17-29-04201, and the Ministry of Science and Higher Education of the Russian Federation within a Government research contract with the Federal Scientific Research Centre "Crystallography and Photonics" of the Russian Academy of Sciences.

REFERENCES

1. A. N. Shcheglov and N. B. Selivanova, *Greek Amphoraes,* Ed. by V. I. Kats and S. Yu. Monakhov (Izd-vo Saratov Gos. Univ., Saratov, 1992), p. 32 [in Russian].
2. A. O. Shepard, *Ceramics for Archaeologists* (Carnegie Inst., Washington, 1956).
3. Y. Garlan and H. Kara, *Les Timbres Céramiques Sinopéens sur Amphores et sur Tuiles Trouvés à Sinope. Présentation et Catalogue* (AnatAnt, Paris, 2004).
4. D. Kassab Tezgör, *Historique et Présentation des Fouilles de l'Atelier de Demirci* (AnatAnt, Paris, 2009).
5. I. B. Zeest, *Bosporus Ceramic Vessels. Materials and Studies on the Archaeology of the Soviet Union,* No. 83 (Nauka, Moscow, 1960) [in Russian].
6. N. F. Fedoseev, Antichnyi Mir Arkheol., No. 14, 339 (2010).
7. V. I. Kats, Ceramic Stamps of Tauric Chersonese, Ed. by S. Yu. Monakhov (Izd-vo Saratov Gos. Univ., Saratov, 1994) [in Russian].
8. V. I. Molodin and L. N. Myl'nikova, Samarskii Nauch. Vestn., No. 3 (12), 122 (2015).
9. V. O. Koz'minykh, I. N. Ganebnykh, O. S. El'tsov, and A. A. Kruglova, Privolzhskii Nauch. Vestn., No. 3–1 (43), 8 (2015).
10. A. Hein, H. Mommsen, and J. Maran, J. Archaeol. Sci., No. 26 (8), 1053 (1999).
11. M. J. Feliu, M. C. Edreira, and J. Martin, Anal. Chim. Acta **502** (2), 241 (2004).
12. D. N. Papadopoulou, M. Lalia-Kantouri, N. Kantiranis, and J. A. Stratis, J. Therm. Anal. Calorim. **84** (1), 39 (2006).
13. P. Bastie, B. Hamelin, F. Fiori, et al., Measur. Sci. Tech., No. 17, L1 (2006).
14. J. Riederer, Hyperfine Interact., No. 154, 143 (2004).
15. A. V. Bakhtiyarov, *X-Ray Spectroscopic Fluorescent Analysis in Geology and Geochemistry* (Nedra, Moscow, 1985) [in Russian].
16. A. Iordanidis, J. Garcia-Guinea, and G. Karamitrou-Mentessidi, Mater. Charact., No. 60, 292 (2009).
17. V. O. Ponomarenko, D. A. Sarychev, and L. N. Vodolazhskaya, Vestn.Yuzhn. Nauch. Tsentra Ross. Akad. Nauk, **8** (1), 9 (2012).
18. V. E. Medvedev and I. V. Filatova, Teor. Prakt. Arkheol. Issled., No. 3 (19), 150 (2017).
19. P. E. Belousov, Yu. I. Bocharnikova, and N. M. Boeva, Vestn. RUDN, No. **4**, 94 (2015).
20. V. A. Drebushchak, L. N. Myl'nikova, and T. N. Drebushchak, *Physicochemical Study of Ceramics from the Chronologically Transitional (Bronze–Iron Age) Sites* (Izd-vo SO RAN, Novosibirsk, 2006) [in Russian].
21. L. Maritan, L. Nodari, C. Mazzoli, et al., Appl. Clay Sci. **31** (1–2), 1 (2006).
22. G. Cultrone, C. Rodriguez-Navarro, E. Sebastian, et al., Eur. J. Mineral. **13**, 621 (2001).
23. R. Scarpelli, Robin. J. H. Clark, and A. M. De Francesco, Spectrochim. Acta A **120**, 60 (2014).
24. M. Maggetti, C. Neururer, and D. Ramseyer, Appl. Clay Sci. **53**, 500 (2011).
25. M. T. Kasymova and G. T. Oruzbaeva, Vestn. KRSU **17** (8), 112 (2017).
26. I. M. Potasheva and S. A. Svetov, Tr. Karel'skogo Nauch. Tsentra Ross. Akad. Nauk, No. **4**, 136 (2013).
27. I. M. Potasheva and S. A. Svetov, Proc. Petrozavodsk State Univ., No. 4 (141), 71 (2014).
28. I. M. Summanen and S. A. Svetov, Uch. Zap. Petrozavodskogo Gos. Univ., No. 1 (162), 18 (2017).
29. N. C. Little, L. J. Kosakowsky, R. J. Speakman, et al., J. Radio Anal. Nucl. Chem. **262** (1), 103 (2004).
30. A. Hein, V. Georgopoulou, E. Nodarou, et al., J. Archaeol. Sci., No. 35, 1049 (2008).
31. I. M. Potasheva, S. Yu. Chazhengina, and S. A. Svetov, Uch. Zap. Petrozavodskogo Gos. Univ., No. 8 (137), 44 (2013).
32. V. Georgopoulou, *Ph. D. Thesis* (University of Athens, 2006) [in Greek]).
33. A. V. Mandrykina, D. N. Khmelenin, N. N. Kolobylina, et al., Crystallogr. Rep. **63** (5), 849 (2018).
34. V. G. Kon, P. A. Prosekov, A. Yu. Seregin, et al., Crystallogr. Rep. **64** (1), 24 (2019).
35. V. A. Sole, E. Papillon, M. Cotte, et al., Spectrochim. Acta B **62**, 63 (2007).
36. K. Chinnathambi, *Miniflex Guidance* (2018).
37. *PDXL 2: Advanced Integrated X-ray Powder Diffraction Suite,* The Rigaku J. **28** (1), 29 (2012).
38. V. Petricek, M. Dusek, and L. Palatinus, Z. Kristallogr. **229** (5), 345 (2014).
39. D. M. Kheiker, M. V. Koval'chuk, V. N. Korchuganov, et al., Crystallogr. Rep. **52** (6), 1108 (2007).
40. A. P. Hammersley, *FIT2D V9.129 Reference Manual. V3.1* (1998).
41. H. Putz and K. Brandenburg, *Match–Phase Identification from Powder Diffraction. Crystal Impact Software* (2015).
42. C. R. Hubbard, E. H. Evans, and D. K. Smith, J. Appl. Crystallogr. **9** (2), 169 (1976).
43. D. Kutscher, J. D. Wills, and S. M. Ducos, *Thermo Fisher Scientific. Technical Note 43279* (Bremen, Germany). https://assets.thermofisher.com/TFS-Assets/CMD/Technical-Notes/tn-43279-icp-ms-isds-nanparticle-tn43279-en.pdf.
44. I. I. Chaikovskii, A. T. Sirazetdinov, and O. S. Kablinov, Nauch. Chteniya Pamyati P. N. Chirvinskogo, No. 11, 67 (2008).
45. B. Fabbri, S. Gualtieri, and S. Shoval, J. Eur. Ceram. Soc. **34** (7), 1899 (2014).
46. L. Renetal, Appl. Geochem. **56**, 80 (2015).

Translated by Yu. Sin'kov